Journal of Magnetic Resonance Open 10-11 (2022) 100026

Contents lists available at ScienceDirect

Journal of Magnetic Resonance Open

journal homepage: www.sciencedirect.com/journal/journal-of-magnetic-resonance-open

Mechanism of chirp excitation

Sreya Das, Justin Jacob, Navin Khaneja *

System and Control Engineering, IIT Bombay, Powai 400076, India

A B S T R A C T

In design of a chirp inversion pulse, we keep the sweep rate $a \ll \omega_1^2$, where ω_1 is the amplitude of the pulse. This is the adiabaticity condition for the inversion to work. We can convert a chirp inversion pulse to an excitation pulse by keeping the chirp rate high, with $a > \omega_1^2$. To be precise $a = 2.8\omega_1^2$. The analysis of such a pulse breaks the evolution into three phases. The first and third phase are adiabatic phases while the second phase is non-adiabatic. Starting from north pole such a pulse brings the magnetization to equator, however there is a nonuniform phase which depends on the resonance offsets. We show how by following this pulse with a chirp inversion pulse at twice the sweep rate of excitation pulse, we can refocus this uniform phase. We find there is still some phase dispersion. This can be further eliminated by bringing in a second inversion pulse. The combination of these three chirp pulses allows us to excite arbitrary large bandwidth without increasing the peak amplitude of the pulse. Refocusing properties of pair of chirp has been studied before but our description is very different.

1. Introduction

Broadband excitation is a fundamental problem in NMR spectroscopy. The goal is to excite magnetization with resonance offsets lying a certain spectral range due to phenomenon of chemical shifts. Higher spectrometer field strengths provide significantly increased sensitivity and spectral resolution, but the sample must also be excited over a correspondingly expanded range of chemical shift frequencies. Ideally, one would like the excitation profile over the range to be uniform, producing transverse magnetization of constant phase. Keeping pace with steadily increasing field strength is a challenge, given maximum power tolerances of typical RF probes. At a field of 1 GHz, the target bandwidth is 50 kHz for excitation of entire 200 ppm ^{13}C chemical shifts. The required 25 kHz hard pulse exceeds the capabilities of most ^{13}C probes and poses additional problems in phasing the spectra. In ^{19}F NMR, chemical shifts can range over 600 ppm, which requires excitation of different regions of the spectra. Methods that can achieve uniform excitation over the entire bandwidth in ^{19}F NMR, are therefore most desirable. Towards this end, several methods have been developed for broadband excitation/inversion, which have reduced the phase variation of the excited magnetization as a function of the resonance offset. These include composite pulses, adiabatic sequences, polychromatic sequences, phase alternating pulse sequences, optimal control pulse design, and method of multiple frames, [1–12,14–32].

In this paper we study a broadband adiabatic pulse, *Chorus* [26] which gives uniform excitation over unprecedented frequency range, with a uniform phase. *Chorus* is a composite adiabatic pulse. It has a pulse element that produces excitation of magnetization we call it chirp excitation. In this paper, we elucidate the mechanism behind working of chirp excitation [13]. We first develop a three stage model for understanding chirp excitation in NMR. The phase of magnetization resulting from chirp excitation pulse is non-uniform as function of offsets. We then show how a chirp π pulse can be used to refocus the phase of the excitation pulse. The resulting magnetization still has some phase dispersion in it. We show how a combination of two chirp π pulses instead of one can be used to eliminate this dispersion leaving behind a small residual phase dispersion. The pulse sequence presented here allows exciting arbitrary large bandwidths without increasing the peak rf-amplitude. Although methods presented in this paper have appeared elsewhere [3,5,26,32], we present complete analytical treatment that elucidates the working of these methods. The paper further develops the treatment in [13] by providing more elaborate and transparent proofs.

The paper is organized as follows. In Section 2, we present the mechanism behind chirp excitation. In Section 3, we present simulation and experimental results for broadband excitation pulses designed using chirp pulses. We conclude in Section 4, with discussion and outlook.

2. Theory

Let

$$\Omega_x = \begin{bmatrix} 0 & 0 & 0 \\ 0 & 0 & -1 \\ 0 & 1 & 0 \end{bmatrix}, \quad \Omega_y = \begin{bmatrix} 0 & 0 & 1 \\ 0 & 0 & 0 \\ -1 & 0 & 0 \end{bmatrix}, \quad \Omega_z = \begin{bmatrix} 0 & -1 & 0 \\ 1 & 0 & 0 \\ 0 & 0 & 0 \end{bmatrix}.$$

* Corresponding author.
E-mail address: nkhaneja@sc.iitb.ac.in (N. Khaneja).

https://doi.org/10.1016/j.jmro.2021.100026
Received 4 September 2021; Received in revised form 3 December 2021; Accepted 7 December 2021
Available online 9 December 2021

denote generator of rotations around x, y, z axis respectively. A x-rotation by flip angle θ is $\exp(\theta\Omega_x)$.

2.1. Chirp inversion

Before we present the theory behind chirp excitation, it is worthwhile to recapitulate the basics of chirp inversion, and establish needed notation for the subsequent paper. We assume our resonance offsets are in the range $[-B, B]$ and we sweep through them with instantaneous frequency $\omega(t) = -A + at$ going from $[-A, A]$, such that $\omega(t) = \dot{\phi}(t)$, with the phase of the rf field $\phi(t) = -At + \frac{1}{2}at^2$ and a is the sweep rate as shown in Fig. 1. The Bloch equation takes the form

$$\dot{X} = \left(\omega_0\Omega_z + \omega_1\cos\phi\Omega_x + \omega_1\sin\phi\Omega_y\right)X, \tag{1}$$

where X is the Bloch vector, ω_0 the resonance offset and ω_1 the strength of rf-field. In the frame of phase ϕ defined as $Y = \exp(-\phi(t)\Omega_z)X$, we have

$$\dot{Y} = ((\omega_0 - \omega(t))\Omega_z + \omega_1\Omega_x)Y, \tag{2}$$

which we rewrite as,

$$\dot{Y} = \omega_{\text{eff}}(\cos\theta(t)\Omega_z + \sin\theta(t)\Omega_x)Y, \tag{3}$$

where $\omega_{\text{eff}} = \sqrt{(\omega_0 - \omega(t))^2 + \omega_1^2}$ and $\tan\theta(t) = \frac{\omega_1}{\omega_0 - \omega(t)}$. Going in frame of θ, i.e. $Z(t) = \exp(-\theta(t)\Omega_y)Y(t)$ we get

$$\dot{Z} = \left(-\dot{\theta}\Omega_y + \omega_{\text{eff}}\Omega_z\right)Z. \tag{4}$$

If $\omega_{\text{eff}} \gg \dot{\theta}$ it averages $\dot{\theta}$ and we get $Z(T) = \exp(\int_0^T \omega_{\text{eff}}\Omega_z)Z(0)$. Lets look at the averaging condition.

$$\dot{\theta}(t) = \frac{a\omega_1}{\omega_{\text{eff}}^2}.$$

$\omega_{\text{eff}} \gg \dot{\theta}$ is satisfied when $a \ll \omega_{\text{eff}}^2$, this is the adiabaticity condition which is always true if $a \ll \omega_1^2$. Under this averaging we get

$$Y(T) = \exp\left(\theta(T)\Omega_y\right)\exp\left(\int_0^T \omega_{\text{eff}}\Omega_z\right)\exp\left(-\theta(0)\Omega_y\right)Y(0). \tag{5}$$

Assuming we start sufficiently off-resonant $(A - B \gg \omega_1)$ $\theta(0) \sim 0$, we have

$$X(T) = \exp(\phi(T)\Omega_z)\exp\left(\theta(T)\Omega_y\right)\exp\left(\int_0^T \omega_{\text{eff}}\Omega_z\right)\exp\left(-\phi(0)\Omega_z\right)X(0). \tag{6}$$

Since $\phi(0) = \phi(T) = 0$ we have

$$X(T) = \exp\left(\theta(T)\Omega_y\right)\exp\left(\int_0^T \omega_{\text{eff}}\Omega_z\right)X(0).$$

We start from $X(0) = \begin{bmatrix} 0 \\ 0 \\ 1 \end{bmatrix}$. Then for $A - B$ sufficiently large compared to ω_1, $\theta(T) = \pi$, we have

$$X(T) = \exp\left(\theta(T)\Omega_y\right)X(0) = \begin{bmatrix} 0 \\ 0 \\ -1 \end{bmatrix}. \tag{7}$$

We achieve adiabatic inversion over the range of resonance offsets. The key is the adiabaticity condition $a \ll \omega_{\text{eff}}^2$.

2.2. Chirp excitation

In chirp excitation, we donot have the adiabaticity condition $a \ll \omega_{\text{eff}}^2$ true at all times. Infact we keep the sweep rate larger say $a = \beta^2\omega_1^2$ such that $\beta > 1$. Then when we sweep through resonance ω_0, outside the range $[\omega_0 - \beta\omega_1, \omega_0 + \beta\omega_1]$, it is still true that the $\omega_{\text{eff}}^2 > a$ and the evolution is adiabatic, however in the range $[\omega_0 - \beta\omega_1, \omega_0 + \beta\omega_1]$, the evolution is non adiabatic. We can divide the pulse sequence into three phases, when we sweep from -A to $\omega_0 - \beta\omega_1$ we call it phase I. When we sweep $[\omega_0 - \beta\omega_1, \omega_0 + \beta\omega_1]$, we call it phase II and finally we sweep from $\omega_0 + \beta\omega_1$ to A we call it phase III. This is as shown in Fig. 2. Let $\beta = \cot\theta_0$, then

A chirp excitation pulse is understood as concatenation of three effective rotations

$$\underbrace{\exp\left(\theta_0\Omega_y\right)}_{III}\ \underbrace{\exp(\alpha\Omega_x)}_{II}\ \underbrace{\exp\left(\theta_0\Omega_y\right)}_{I}, \tag{8}$$

which satisfy $\cos\alpha = \tan^2\theta_0$. Lets see how these effective rotations arise.

In phase I of the pulse, the evolution is adiabatic as $\omega_{\text{eff}} \geq \sqrt{\beta^2\omega_1^2 + \omega_1^2} = \sqrt{1 + \beta^2}\omega_1$ and the Y vector as in previous section follows the Eq. (2) and evolves for time t_1 as in Eq. (5)

$$Y(T) = \exp\left(\theta_0\Omega_y\right)\exp\left(\int_0^{t_1} \omega_{\text{eff}}\Omega_z\right)Y(0) = \begin{bmatrix} \sin\theta_0 \\ 0 \\ \cos\theta_0 \end{bmatrix}. \tag{9}$$

During the phase *II* of the pulse the evolution is non-adiabatic, frequency $\omega - \omega_0$ is swept over the range $[-\beta\omega_1,\ \beta\omega_1]$ in time $t_2 = \frac{2\beta\omega_1}{\beta^2\omega_1^2}$ with $\alpha = \omega_1 t_2 = \frac{2}{\beta}$ and for $\frac{2}{\beta}$ not very larger than 1, we can approximate the evolution of Y vector in this phase II by directly integrating equation Eq. (2) and the evolution is governed by the propagator

$$\sim \exp\left(\int_0^{\alpha/\omega_1} (\omega_0 - \omega)\Omega_z + \omega_1\Omega_x\right)dt = \exp(\alpha\Omega_x). \tag{10}$$

This produces the evolution

$$\begin{bmatrix} \sin\theta_0 \\ 0 \\ \cos\theta_0 \end{bmatrix} \rightarrow \begin{bmatrix} \sin\theta_0 \\ -\cos\theta_0\sin\alpha \\ \cos\theta_0\cos\alpha \end{bmatrix}. \tag{11}$$

Finally, during phase *III*, the frequency is swept from $\omega_1\cot\theta_0$ to a large positive offset A and this evolution is adiabatic. This produces the transformation of Y vector as

$$\exp\left(-\int_{III} \omega_{\text{eff}}(t)\ dt\ \Omega_z\right)\exp\left(\theta_0\ \Omega_y\right)\begin{bmatrix} \sin\theta_0 \\ -\cos\theta_0\sin\alpha \\ \cos\theta_0\cos\alpha \end{bmatrix}. \tag{12}$$

To see this, evolution of the Y vector as in Eq. (5) is

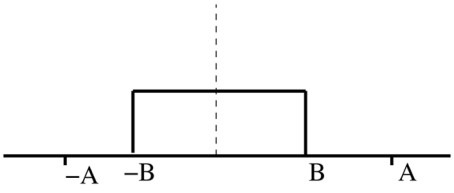

Fig. 1. The figure shows the offsets in range $[-B, B]$ and the sweep of chirp from $[-A, A]$ at sweep rate a.

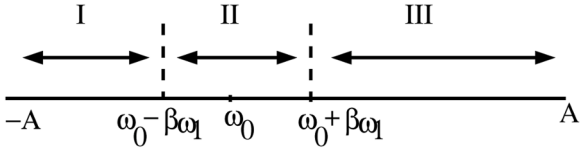

Fig. 2. The figure shows the three phases of excitation pulse.

$$Y(T) = \exp\big(\theta(T)\Omega_y\big)\exp\left(\int_{III}\omega_{\text{eff}}\Omega_z\right)\exp\big(-\theta(0)\Omega_y\big)Y(0). \tag{13}$$

Here $\theta(0) = \pi - \theta_0$ and $\theta(T) = \pi$ giving us Eq. (12).

Now for this to be an excitation, the z coordinate should vanish, which means, if in Eq. (12) we apply the $\exp(\theta_0\ \Omega_y)$ rotation and observe the z coordinate, the condition for z coordinate to go to 0 is,

$$\cos^2\theta_0\cos\alpha = \sin^2\theta_0. \tag{14}$$

$$\tan^2\theta_0 = \cos\alpha. \tag{15}$$

which gives

$$\frac{1}{\beta^2} = \cos\frac{2}{\beta}, \tag{16}$$

which gives $\beta^2 = 2.81$.

Hence the sweep rate is $a = 2.81\omega_1^2$ for the chirp pulse to be an excitation. Figure 3 shows how the effective field and magnetization evolves in three phases of the excitation pulse.

2.3. Simulation of three phases of excitation pulse

We simulate the trajectory for three phases of the pulse sequence. We take resonance offset as 0. For $\beta^2 = 2.8$, we sweep for $A = 75$ units from $-A$ to $\beta\omega_1$ with $\omega_1 = 1$ unit. Recall sweep from $-A$ to $-\beta\omega_1$ is phase I of the sequence and from $-\beta\omega_1$ to $\beta\omega_1$ is phase 2. We find the first phase of trajectory is coiled as it adiabatically follows the effective field. This is seen in top view of Bloch sphere as the initial part of trajectory which is coiled in top panel in Fig. 4. Phase two is a rotation around x axis which is seen as the second part of the trajectory seen in top panel in Fig. 4. The two phases are also shown in side view of the sphere in center panel in Fig. 4. The bottom panel also shows the third phase which in a evolution around y axis followed by evolution around z axis. We see this evolution around z axis as winding of the trajectory around the equator in bottom panel in Fig. 4.

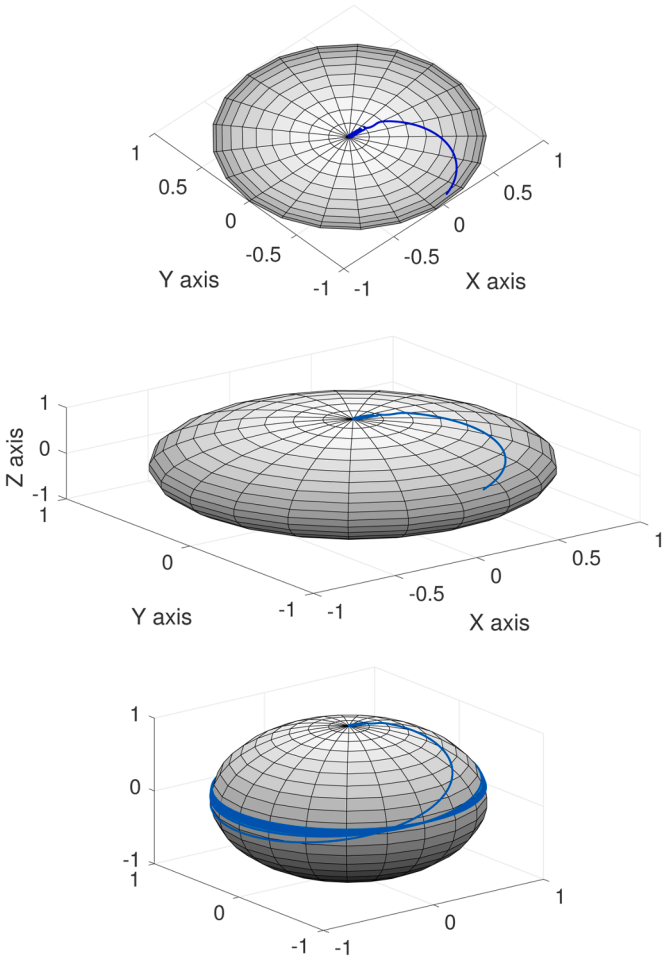

Fig. 4. The Fig simulates the trajectory of three phases of the pulse sequence. Top and middle panel shows first two phase of the pulse sequence. Bottom panel shows all phases of the chirp excitation pulse .

2.4. Refocussing chirp excitation

The factor $\exp(-\int_{III}\omega_{\text{eff}}(t)\ dt\ \Omega_z)$ in Eq. (12) dephases the magnetization on the equator. Our goal now is the refocus this magnetization.

For this we follow the chirp excitation pulse with chirp inversion pulse with sweep rate twice of excitation i.e. $2a$ and amplitude ω_2 satisfying the adiabaticity condition $\omega_2^2 \gg 2a$. The π pulse evolution is

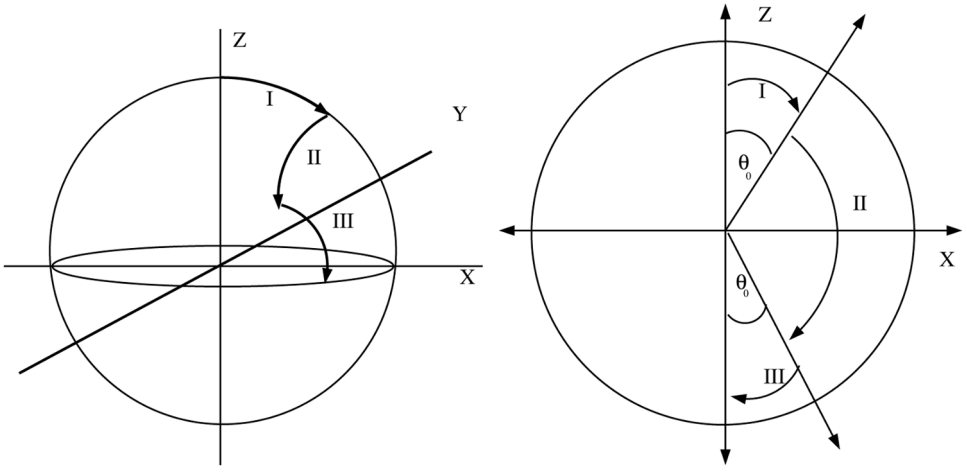

Fig. 3. The *right panel* shows the effective field for the chirp excitation. The effective field starts along z axis and after phase I is rotated by θ_0. After phase *II*, it makes angle of θ_0 with $-z$ axis and finally at end of phase III ends up at the $-z$ axis. The *left panel* shows how magnetization initially along z axis evolves in three stages in frame of phase $\phi(t)$ as in Eq. (2). It is rotated along y axis in phase I by angle θ_0 and then along x axis by angle α in phase II and finally along y axis by θ_0 in phase III.

$$\exp(\pi\Omega_y)\exp\left(\int_0^{\frac{T}{2}}\omega'_{\text{eff}}\Omega_z\right). \tag{17}$$

where ω'_{eff} is effective field in the π pulse. The evolution of the net phase due to π pulse and $\frac{\pi}{2}$ pulse from Eq. (12) is

$$\int_0^{\frac{T}{2}}\omega'_{\text{eff}}dt - \int_{III}\omega_{\text{eff}}\ dt, \tag{18}$$

$$\int_0^{\frac{T}{2}}\omega'_{\text{eff}}dt = \int_0^{\frac{T}{2}}\omega'_{\text{eff}}(-A+2at)dt, \tag{19}$$

substituting $\omega = -A+2at$, we get

$$\int_0^{\frac{T}{2}}\omega'_{\text{eff}}dt = \frac{1}{2a}\int_{-A}^{A}\omega'_{\text{eff}}(\omega)d\omega. \tag{20}$$

For $\omega-\omega_0 > \omega_2$ we can expand

$$\omega'_{\text{eff}} = \sqrt{(\omega-\omega_0)^2+\omega_2^2} \sim \omega-\omega_0+\frac{1}{2}\frac{\omega_2^2}{\omega-\omega_0}. \tag{21}$$

This gives $\frac{1}{4a}\omega_2^2\ln\frac{(A^2-\omega_0^2)}{\omega_2^2}$. Maximum dispersion happens when $\omega_0 = 0$ vs $\omega_0 = B$. If we plug the two values and subtract to get total phase dispersion, we get

$$\frac{1}{4a}\omega_2^2\ln\frac{(A^2-B^2)}{A^2} = \frac{1}{4a}\omega_2^2\ln\left(1-\frac{B^2}{A^2}\right). \tag{26}$$

There is dispersion due to the term

$$\int_{\omega_0+\omega_2}^{A}\frac{1}{2}\frac{\omega_1^2}{\omega-\omega_0}d\omega$$

which gives $\frac{1}{2a}\omega_1^2\ln\frac{(A-\omega_0)}{\omega_2}$. Maximum dispersion due to this term happens when $\omega_0 = -B$ vs $\omega_0 = B$ and this contributes a phase error $\frac{1}{2a}\omega_1^2\ln\frac{1-\frac{B}{A}}{1+\frac{B}{A}}$. Both these dispersions are small in the limit $B \ll A$. In nutshell we cancel the principle phase dispersion of $\omega_0\frac{T}{2}$ by free evolution. The remaining dispersion can be made arbitrary small. This is the pulse sequence shown in Fig. 5A.

We can further cancel the dispersion $\frac{1}{4a}\omega_2^2\ln 1-\frac{B^2}{A^2}$ by doing the three pulse sequence as shown in Fig. 6A. The pulse sequence consists of a $\frac{\pi}{2}$ excitation pulse of duration T followed by a π inversion pulse of duration

$$\begin{aligned}\frac{1}{2a}\int_{-A}^{A}\omega'_{\text{eff}}(\omega)d\omega &= \frac{1}{2a}\left(\int_{-A}^{\omega_0-\omega_2}\omega'_{\text{eff}}(\omega)d\omega+\int_{\omega_0-\omega_2}^{\omega_0+\omega_2}\omega'_{\text{eff}}(\omega)d\omega+\int_{\omega_0+\omega_2}^{A}\omega'_{\text{eff}}(\omega)d\omega\right)\\ &= \frac{1}{2a}\int_{-A}^{\omega_0-\omega_2}\left((\omega_0-\omega)+\frac{1}{2}\frac{\omega_2^2}{\omega_0-\omega}\right)d\omega+\int_{\omega_0-\omega_2}^{\omega_0+\omega_2}\omega'_{\text{eff}}(\omega)d\omega+\int_{\omega_0+\omega_2}^{A}\left((\omega-\omega_0)+\frac{1}{2}\frac{\omega_2^2}{\omega-\omega_0}\right)d\omega.\end{aligned} \tag{22}$$

T both at same sweep rate and finally a free evolution for time $\frac{T}{2}$ followed by a π inversion pulse of duration $\frac{T}{2}$ at twice the chirp rate. The ratio of amplitude of last π pulse to center π pulse is $\sqrt{2}$. The first $\frac{\pi}{2}$ excitation

$$\int_{III}\omega_{\text{eff}}\ dt = \frac{1}{a}\left(\int_{\omega_0+\beta\omega_1}^{\omega_0+\omega_2}\omega_{\text{eff}}(\omega)d\omega+\int_{\omega_0+\omega_2}^{A}\omega_{\text{eff}}(\omega)d\omega\right) \tag{23}$$

$$= \frac{1}{a}\left(\int_{\omega_0+\beta\omega_1}^{\omega_0+\omega_2}\omega_{\text{eff}}(\omega)d\omega+\int_{\omega_0+\omega_2}^{A}\left((\omega-\omega_0)+\frac{1}{2}\frac{\omega_1^2}{\omega-\omega_0}\right)d\omega\right). \tag{24}$$

Observe term $\int_{\omega_0-\omega_2}^{\omega_0+\omega_2}\omega'_{\text{eff}}(\omega)d\omega$ has no dispersion, it is same for all ω_0, so we neglect it and replace it with $\int_{\omega_0-\omega_2}^{\omega_0+\omega_2}(\omega_0-\omega)d\omega$ which is zero by construction. Similarly term $\int_{\omega_0+\beta\omega_1}^{\omega_0+\omega_2}\omega_{\text{eff}}(\omega)d\omega$ has no dispersion and we omit it. Then collecting terms linear in ω we get

$$\begin{aligned}&\frac{1}{2a}\int_{-A}^{A}\omega'_{\text{eff}}(\omega)d\omega-\frac{1}{a}\int_{III}\omega_{\text{eff}}\ d\omega\\ &= \tfrac{1}{2a}\quad\int_{-A}^{\omega_0-\omega_2}\omega_0-\omega+\int_{\omega_0-\omega_2}^{\omega_0+\omega_2}\omega_0-\omega+\int_{\omega_0+\omega_2}^{A}\omega_0-\omega\\ &= \frac{1}{2a}\int_{-A}^{A}\omega_0-\omega\ \ d\omega,\end{aligned} \tag{25}$$

again $\frac{1}{2a}\int_{-A}^{A}\omega d\omega$ is a constant and has no ω_0 dispersion in it. Leaving behind $\frac{1}{2a}\int_{-A}^{A}\omega_0\ d\omega = \frac{\omega_0 T}{2}$. If we follow the π pulse with free evolution by $\frac{T}{2}$, we cancel this linear term. The π pulse evolution is

$$\exp(\pi\Omega_y)\exp\left(\int_0^{\frac{T}{2}}\omega'_{\text{eff}}\Omega_z\right),$$

the evolution $\exp(\pi\Omega_y)$ negates the free evolution leading to cancellation just mentioned.

How about contributions from terms like

$$\frac{1}{2a}\quad\int_{-A}^{\omega_0-\omega_2}\frac{1}{2}\frac{\omega_2^2}{\omega_0-\omega}d\omega+\int_{\omega_0+\omega_2}^{A}\frac{1}{2}\frac{\omega_2^2}{\omega-\omega_0}d\omega.$$

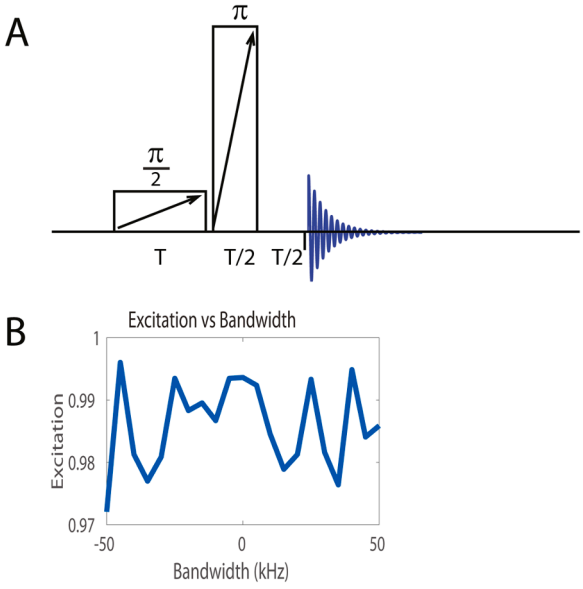

Fig. 5. Fig. A shows the pulse sequence with a $\frac{\pi}{2}$ excitation pulse of duration T followed by a π inversion pulse of duration $\frac{T}{2}$ at twice the sweep rate and finally a free evolution for time $\frac{T}{2}$. Fig. B shows simulation results of sequence in Fig. A, where we choose amplitude of π pulse as 5 kHz and $\frac{\pi}{2}$ pulse as 1 kHz. The Bandwidth $B/2\pi = 50$ kHz and $A/2\pi = 250$ kHz. Sweep rate $a = 2.8\times(2\pi\ kHz)^2$ and time $T = 28.42$ ms. Total duration of the pulse is 56.84 ms. We show the excitation which is 0 phase corrected to be x excitation.

pulse contributes a phase $-\int_{III}\omega_{\text{eff}}dt$ as before, the phase due to next π pulse is

$$\int_0^T \omega'_{\text{eff}}dt = \frac{1}{a}\int_{-A}^{A}\omega'_{\text{eff}}(\omega)d\omega, \tag{27}$$

and the phase due to last π pulse is

$$-\int_0^{T/2}\omega''_{\text{eff}}dt = -\frac{1}{2a}\int_{-A}^{A}\omega''_{\text{eff}}(\omega)d\omega. \tag{28}$$

To understand negative sign above if we write the evolution of two π pulses, with free evolution inbetween, it takes the form

$$\exp(\pi\Omega_y)\exp\left(\int_0^{\frac{T}{2}}\omega''_{\text{eff}}\Omega_z\right)\exp\left(\omega_0\frac{T}{2}\Omega_z\right)\exp(\pi\Omega_y)\exp\left(\int_0^{T}\omega'_{\text{eff}}\Omega_z\right), \tag{29}$$

which can be written as

$$\exp\left(-\int_0^{\frac{T}{2}}\omega''_{\text{eff}}\Omega_z\right)\exp\left(-\omega_0\frac{T}{2}\Omega_z\right)\exp\left(\int_0^{T}\omega'_{\text{eff}}\Omega_z\right).$$

Let the amplitude of last pulse be ω_2 then center π pulse has amplitude $\frac{\omega_2}{\sqrt{2}}$.

Expanding these two phases we have $\frac{1}{a}\int_{-A}^{A}\omega'_{\text{eff}}(\omega)d\omega =$

$$\frac{1}{a}\int_{-A}^{\omega_0-\omega_2}\left((\omega_0-\omega)+\frac{1}{4}\frac{\omega_2^2}{\omega_0-\omega}\right)d\omega+\int_{\omega_0-\omega_2}^{\omega_0+\omega_2}\omega'_{\text{eff}}(\omega)d\omega + \int_{\omega_0+\omega_2}^{A}\left((\omega-\omega_0)+\frac{1}{4}\frac{\omega_2^2}{\omega-\omega_0}\right)d\omega, \tag{30}$$

and due to last pulse

$\frac{1}{2a}\int_{-A}^{A}\omega''_{\text{eff}}(\omega)d\omega =$

$$\frac{1}{2a}\int_{-A}^{\omega_0-\omega_2}\left((\omega_0-\omega)+\frac{1}{2}\frac{\omega_2^2}{\omega_0-\omega}\right)d\omega+\int_{\omega_0-\omega_2}^{\omega_0+\omega_2}\omega''_{\text{eff}}(\omega)d\omega + \int_{\omega_0+\omega_2}^{A}\left((\omega-\omega_0)+\frac{1}{2}\frac{\omega_2^2}{\omega-\omega_0}\right)d\omega. \tag{31}$$

combining the two we get

$$\frac{1}{2a}\int_{-A}^{\omega_0-\omega_2}(\omega_0-\omega)d\omega+\int_{\omega_0-\omega_2}^{\omega_0+\omega_2}\omega_0-\omega+\int_{\omega_0+\omega_2}^{A}(\omega-\omega_0)d\omega, \tag{32}$$

where we have again omitted terms that donot have dispersion and added a zeros as $\int_{\omega_0-\omega_2}^{\omega_0+\omega_2}\omega_0-\omega$. The result is precisely what we had in last analysis from π pulse except the dispersion of the form $\frac{\omega_2^2}{\omega-\omega_0}$ have cancelled. The linear dispersion again combines with $-\int_{III}\omega_{\text{eff}}$ to give $\omega_0 T/2$, which is cancelled by free evolution for time $\frac{T}{2}$. Thus combination of two π pulses cancels the dispersion as in Eq. (26).

3. Simulation and experiments

In Fig. 5A, we choose amplitude of π pulse as 5 kHz and $\frac{\pi}{2}$ pulse as 1 kHz. The bandwidth $B/2\pi = 50$ kHz and $A/2\pi = 250$ kHz. Sweep rate $a = 2.8\times(2\pi\ kHz)^2$ and time $T = 28.42$ ms. Total duration of the pulse is 56.84 ms. Figure 5B, shows the x-coordinate of the excited magnetization, after a zero order phase correction.

Finally, in Fig. 6A, we taper the edges of chirp pulse so that we don't have to sweep very far. We choose peak Amplitude of last π pulse as 20 kHz, center π pulse as $\frac{20}{\sqrt{2}}$ kHz and $\frac{\pi}{2}$ pulse as 4 kHz. The Bandwidth $B/2\pi = 200$ kHz and $A/2\pi = 240$ kHz. Sweep rate $a = 2.8\times(2\pi\times 4\ kHz)^2$ and time $T = 1.7$ ms. Total duration of the pulse sequence is 5.1 ms. Figure 6B, shows the x-coordinate of the excited magnetization, after a zero order phase correction.

Experimental realization of this pulse sequence in Fig. 6A is done on a 750 MHz spectrometer. Figure 7 shows experimental excitation profiles of residual HDO signal in a sample of 99.5% D_2O, as a function of resonance offset, after application of the pulse sequence in Fig. 6A. The offset is varied in increments of 20 kHz, over a range of 400 kHz ([-200, 200] kHz) around the proton resonance at 4.7 ppm. The peak amplitude of the pulse is 20 kHz. We find uniform excitation experimentally.

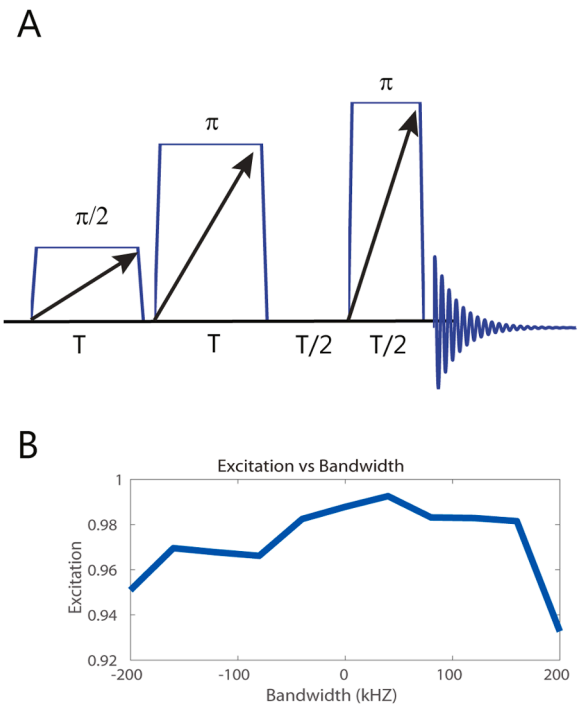

Fig. 6. Fig. A shows the pulse sequence with a $\frac{\pi}{2}$ excitation pulse of duration T followed by a π inversion pulse of duration T both at same sweep rate and finally a free evolution for time $\frac{T}{2}$ followed by a π inversion pulse of duration $\frac{T}{2}$ at twice the chirp rate. The amplitude at ends of chirp pulses is tapered to minimize sweep width. The ratio of peak amplitude of last π pulse to center π pulse is $\sqrt{2}$. Fig. B shows the excitation profile after a zero order phase correction of the pulse sequence in Fig. A. We choose peak amplitude of last π pulse as 20 kHz, center π pulse as $\frac{20}{\sqrt{2}}$ kHz and $\frac{\pi}{2}$ pulse as 4 kHz. The bandwidth $B/2\pi = 200$ kHz and $A/2\pi = 240$ kHz. Sweep rate $a = 2.8\times(2\pi\times 4\ kHz)^2$ and time $T = 1.7$ ms. Total duration of the pulse sequence is 5.1 ms.

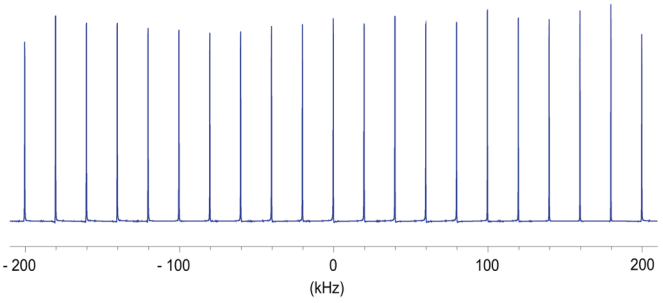

Fig. 7. Above figure shows experimental excitation profiles of residual HDO signal in a sample of 99.5% D_2O, as a function of resonance offset, after application of the pulse sequence in Fig. 6A. The offset is varied in increments of 20 kHz, over a range of 400 kHz as in Fig. 6B.

This pulse sequence appears as CHORUS in [26]. Here we provide details of the working of this sequence.

4. Conclusion

In this paper we studied the broadband excitation pulse CHORUS

[26]. CHORUS is a composite pulse with three pulse elements. In this paper we showed the three pulse elements of CHORUS can be broken as an initial excitation pulse followed by two Refocusing pulse elements. We analyze the excitation pulse by developing a three stage model. The three stage model has two adiabatic phases and one non-adiabatic phase. The resulting excitation pulse has a nonuniform excitation phase. We then showed how a chirp π pulse can be used to refocus the phase of the chirp excitation pulse. The resulting magnetization still had some phase dispersion in it. We then showed how a combination of two chirp π pulses instead of one can be used to eliminate this dispersion, leaving behind a small residual phase dispersion. The excitation pulse sequence presented here allows exciting arbitrary large bandwidths without increasing the peak rf-amplitude. They are expected to find immediate application in ^{19}F NMR. Although methods presented in this paper have appeared elsewhere [3,5,26], we present complete analytical treatment that elucidates the working of these methods. It is worth mentioning that the excitation bandwidths achieved by the present approach far exceeds those that have been possible with recent optimal control methods [15,28,29]. Future work in direction is to use these methods to develop general purpose rotation pulses, like a broadband $\left(\frac{\pi}{2}\right)_x$ rotation.

Declaration of Competing Interest

I would like to declare that there are no known conflicts of interest associated with this publication and there has been no significant financial support for this work that could have influenced its outcome.

References

[1] D. Abramovich, S. Vega, Derivation of broadband and narrowband excitation pulses using the Floquet formalism, J. Magn. Reson. Ser. A. 105 (1993) 30–48.
[2] J. Baum, R. Tycko, A. Pines, Broadband and adiabatic inversion of a two level system by phase modulated pulses, Phys. Rev. A 32 (1985) 3435–3447.
[3] J.-M. Böhlen, G. Bodenhausen, Experimental aspects of chirp NMR spectroscopy, J. Magn. Reson. Ser. A 102 (1993) 293–301.
[4] J.M. Böhlen, I. Burghardt, M. Rey, G. Bodenhausen, Frequency modulated "chirp" pulses for broadband inversion recovery in magnetic resonance, J. Magn. Reson. 90 (1990) 183–191.
[5] J.-M. Böhlen, M. Rey, G. Bodenhausen, Refocusing with chirped pulses for broadband excitation without phase dispersion, J. Magn. Reson. 84 (1989) 191–197.
[6] K.E. Cano, M.A. Smith, A.J. Shaka, Adjustable, broadband, selective excitation with uniform phase, J. Magn. Reson. 155 (2002) 131–139.
[7] V.L. Ermakov, G. Bodenhausen, Broadband excitation in magnetic resonance by self-refocusing doubly frequency-modulated pulses, Chem. Phys. Lett. 204 (1993) 375–380.
[8] V.L. Ermakov, J.M. Böhlen, G. Bodenhausen, Improved schemes for refocusing with frequency-modulated chirp pulses, J. Magn. Reson. Ser. A 103 (1993) 226–229.
[9] R. Freeman, S.P. Kempsell, M.H. Levitt, Radio frequency pulse sequence which compensate their own imperfections, J. Magn. Reson. 38 (1980) 453–479.
[10] M. Garwood, L. Dellabare, The return of the frequency sweep: designing adiabatic pulses for contemporary NMR, J. Magn. Reson. 153 (2001) 155–157.
[11] K. Hallenga, G.M. Lippens, A constant-time ^{13}c-^{1}h HSQC with uniform excitation over the complete ^{13}C chemical shift range, J. Biomol. NMR 5 (1995) 59–66.
[12] T.L. Hwang, P.C.M. van Zijl, M. Garwood, Broadband adiabatic refocusing without phase distortion, J. Magn. Reson. 124 (1997) 250–254.
[13] N. Khaneja, Chirp excitation, J. Magn. Reson 282 (2017) 32–36.
[14] N. Khaneja, A. Dubey, H.S. Atreya, Ultra broadband NMR spectroscopy using multiple rotating frame technique, J. Magn. Reson. 265 (2016) 117–128.
[15] K. Kobzar, T.E. Skinner, N. Khaneja, S.J. Glaser, B. Luy, Exploring the limits of broadbad excitation and inversion: II. Rf-power optimized pulses, J. Magn. Reson. 194 (1) (2008) 58–66.
[16] M.R.M. Koos, H. Feyrer, B. Luy, Broadband excitation pulses with variable RF amplitude-dependent flip angle (RADFA), Magn. Reson. Chem. 53 (11) (2015) 886–893.
[17] E. Kupce, R. Freeman, Wideband excitation with polychromatic pulses, J. Magn. Reson. Ser. A 108 (1994) 268–273.
[18] E. Kupce, R. Freeman, Streched adiabatic pulses for broadband spin inversion, J. Magn. Reson. 117 (1995) 246–256.
[19] M.H. Levitt, Symmetrical composite pulse sequences for NMR population inversion. I. Compensation of radiofrequency field inhomogeneity, J. Magn. Reson. 48 (1982) 234–264.
[20] M.H. Levitt, Composite pulses, Prog. Nucl. Magn. Reson. Spectrosc. 18 (1986) 61–122.
[21] M.H. Levitt, R.R. Ernst, Composite pulses constructed by a recursive expansion procedure, J. Magn. Reson. 55 (1983) 247–254.
[22] D.G. Norris, Adiabatic radiofrequency pulse forms in biomedical nuclear magnetic resonance, Concepts Magn. Reson. 142 (2002) 89–101.
[23] S. Odedra, M.J. Thrippleton, S. Wimperis, Dual-compensated antisymmetric composite refocusing pulses for NMR, J. Magn.Reson. 225 (2012) 81–92.
[24] S. Odedra, S. Wimperis, Use of composite refocusing pulses to form spin echoes, J. Magn. Reson. 214 (2012) 68–75.
[25] Y.J. Park, M. Garwood, Spin echo MRI using $\frac{\pi}{2}$ and π hyperbolic secant pulses, Magn. Reson. Med. (2009) 175–181.
[26] J.E. Power, M. Foroozandeh, R.W. Adams, M. Nilsson, S.R. Coombes, A.R. Phillips, G.A. Morris, Increasing the quantitative bandwidth of NMR measurements, Chem. Commun. 52 (2016) 2916.
[27] A.J. Shaka, A. Pines, Symmetric phase-alternating composite pulses, J. Magn. Reson. 71 (1987) 495–503.
[28] T.E. Skinner, K. Kobzar, B. Luy, M.R. Bendall, W. Bermel, N. Khaneja, S.J. Glaser, Optimal control design of constant amplitude phase-modulated pulses: application to calibration-free broadband excitation, J. Magn. Reson. 179 (2006) 241.
[29] T.E. Skinner, T.O. Reiss, B. Luy, N. Khaneja, S.J. Glaser, Application of optimal control theory to the design of broadband excitation pulses for high-resolution NMR, J. Magn. Reson. 163 (2003) 8–15.
[30] A. Tannús, M. Garwood, Adiabatic pulses, NMR Biomed. 10 (1997) 423–434.
[31] R. Tycho, H.M. Cho, E. Schneider, A. Pines, Composite pulses without phase distortion, J. Magn. Reson. 61 (1985) 90–101.
[32] J.-B. Verstraete, W.K. Myers, M. Foroozandeh, Chirped ordered pulses for ultra-broadband ESR spectroscopy, J. Chem. Phys. 154 (9) (2021) 094201.